

# Supervisory Predictive Control for Long-Term Scheduling of an Integrated Wind/Solar Energy Generation and Water Desalination System

Wei Qi, Jinfeng Liu, and Panagiotis D. Christofides, *Fellow, IEEE*

**Abstract**—In this work, we design a supervisory control system via model predictive control (MPC) for the optimal management and operation of an integrated wind-solar energy generation and reverse-osmosis (RO) water desalination system. The supervisory MPC is able to coordinate the wind and solar subsystems as well as a battery bank to provide enough energy to the RO subsystem so that enough desalinated water can be produced to satisfy the water consumption and storage demands. Optimality considerations on system operation and energy savings are also taken into account via appropriate constraints in the controller formulation. Moreover, in the supervisory MPC design, a two-time-scale property of the dynamics of the integrated system is taken advantage of to improve the computational efficiency of the control problem formulation. Simulations are carried out to illustrate the applicability and effectiveness of the proposed supervisory predictive control design.

**Index Terms**—Model predictive control (MPC), solar energy systems, supervisory control, water desalination systems, wind energy systems.

## I. INTRODUCTION

ALTERNATIVE energy technologies, like wind/solar energy generation systems, are receiving national and worldwide attention owing to the rising rate of consumption of fossil fuels. In particular, drivers for wind/solar energy generation systems are the environmental benefits, reduced investment risk, fuel diversification and energy autonomy. On the other hand, reverse osmosis (RO) membrane desalination has emerged as one of the leading methods for water desalination due to the low cost and energy efficiency of the process (e.g., [1]). Even with advances in reverse osmosis membrane technology, maintaining the desired process conditions is essential to successfully operating an RO desalination system.

Wind and solar energy are attractive choices for providing energy to RO desalination systems for communities in remote areas that have access to sea- or brackish-water. In the past few years, several studies have been done on the integration of wind and solar energy generation systems with RO desalination

systems (e.g., [2]). However, the combination of renewable energy sources and water desalination systems requires addressing challenges in the operation of the integrated system. Specifically, unexpected drops or increases in energy production of a solar or wind energy generation system may require quick start units to cover the shortfall or absorb the unscheduled energy generation. One way to deal with these issues is through the use of integrated energy generation systems using both wind and solar energy.

With respect to previous results on control of wind and solar systems, most of the efforts have focused on control of stand-alone wind (e.g., [3]) or solar systems (e.g., [4]). With respect to the control of RO water desalination systems, a nonlinear model-based control technique was recently proposed to deal with large set-point changes and variations in feed water salinity and was experimentally implemented [5]. In our previous work [6], we proposed a supervisory predictive control method for standalone wind-solar energy generation systems. However, the results obtained in [6] focused on short-term system operation and the approach adopted there cannot be extended to long-term operation because of the high computational burden involved in solving the full, integrated system nonlinear dynamic model.

This work focuses on the design of a supervisory control system for the optimal management and operation of an integrated wind-solar energy generation and RO water desalination system. We propose to design the supervisory control system via model predictive control (MPC) because it can take explicitly into account optimality considerations and handle state and input constraints [7]. In this work, the supervisory MPC coordinates the wind and solar subsystems as well as a battery bank to provide enough energy to the RO subsystem so that enough permeate water can be produced to satisfy the overall water consumption and storage demands. In addition, optimality considerations on system operation and energy savings are also taken into account via appropriate constraints in the controller formulation. To reduce the computational demand of the supervisory MPC optimization problem, a two-time-scale property of the dynamics of the integrated system is taken advantage of to simplify the control problem formulation. Simulations are carried out to illustrate the applicability and effectiveness of the proposed supervisory predictive control design.

## II. INTEGRATED SYSTEM DESCRIPTION

A schematic of the integrated wind/solar/RO system is shown in Fig. 1. This system has two operating modes: standalone operating mode and electrical grid-connected operating mode. In

Manuscript received December 02, 2010; accepted February 09, 2011. Manuscript received in final form February 18, 2011. Date of publication March 22, 2011; date of current version February 01, 2012. Recommended by Associate Editor M. Mattei.

W. Qi and J. Liu are with the Department of Chemical and Biomolecular Engineering, University of California, Los Angeles, CA 90095-1592 USA (e-mail: qiwei.0216@gmail.com; jinfeng@ucla.edu).

P. D. Christofides is with the Department of Chemical and Biomolecular Engineering and the Department of Electrical Engineering, University of California, Los Angeles, CA 90095-1592 USA (e-mail: pdc@seas.ucla.edu).

Digital Object Identifier 10.1109/TCST.2011.2119318

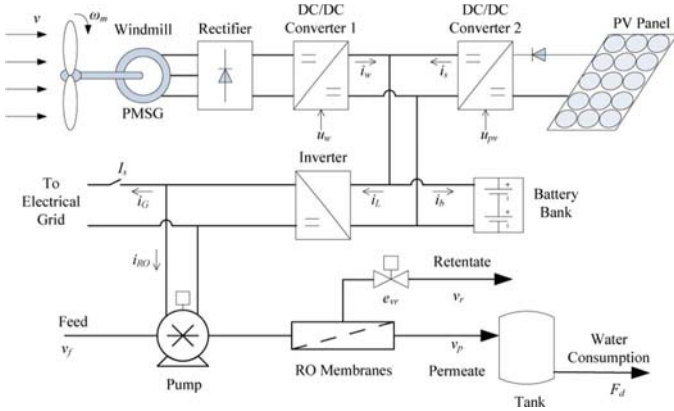


Fig. 1. Integrated wind/solar/RO system.

the standalone operating mode, the wind-solar energy generation system and the battery bank provide energy to the RO water desalination system. In the electrical grid-connected operating mode, the wind-solar energy generation system as well as the battery bank provide energy to the RO water desalination system, and the wind-solar system also sends, if the generation capacity permits, extra energy produced to the electrical grid.

### A. Energy Generation System Description

In the energy generation system, there are three subsystems: a wind generation subsystem, a solar generation subsystem and a lead-acid battery bank.

In the wind generation subsystem, there is a windmill, a multipolar permanent-magnet synchronous generator (PMSG), a rectifier, and a DC/DC converter. The converter is used to control indirectly the operating point of the wind turbine by commanding the voltage on the PMSG terminals. The dynamic behavior of the wind generation subsystem can be characterized by three nonlinear ordinary differential equations (ODEs) involving the quadrature current,  $i_q$ , the direct current,  $i_d$ , in a rotor reference frame and the electrical angular speed,  $\omega_e$ . For the detailed mathematic description of the wind subsystem, please refer to [8]. The power generated by the wind subsystem can be expressed as follows:

$$P_w = i_w v_b \quad (1)$$

where  $i_w = (\pi)/(2\sqrt{3})\sqrt{i_q^2 + i_d^2}u_w$  denotes the current injected to the DC bus by the wind subsystem,  $v_b$  is the voltage on the battery bank terminals, and  $u_w$  is the control signal (duty cycle of the DC/DC converter).

In the solar subsystem, there is a photo-voltaic (PV) panel array and a half-bridge buck DC/DC converter. Similar to the wind subsystem, the converter is used to control the operating point of the PV panels. The dynamic behavior of the solar generation subsystem can be characterized by two nonlinear ODEs involving the voltage level on the PV panel array terminals,  $v_{pv}$ , and the current injected into the DC bus,  $i_s$ . For the detailed mathematic description of the solar subsystem, please refer to

[9]. The power injected into the DC bus by the solar subsystem can be computed by

$$P_s = i_s v_b. \quad (2)$$

Note that this power indirectly depends on the duty cycle of the half-bridge buck DC/DC converter,  $u_{pv}$ , which is the manipulated input for the solar subsystem.

The battery bank is modeled as a voltage source  $E_b$  connected in series with a resistance  $R_b$  and a capacitance  $C_b$ . The DC bus voltage can be written as follows:

$$v_b = E_b + v_c + i_b R_b \quad (3)$$

where  $i_b$  is the current across the battery bank,  $v_c$  is the voltage in capacitor  $C_b$ , and its dynamics is as follows:

$$\dot{v}_c = \frac{1}{C_b} i_b. \quad (4)$$

The state of charge (SOC) of the battery bank  $s_b$  can be calculated as follows:

$$s_b = \frac{Q_c}{Q_c^{\max}} = \frac{v_c}{v_c^{\max}} \quad (5)$$

where  $Q_c^{\max}$  is the maximum capacity of the capacitor corresponding to the maximum voltage,  $v_c^{\max}$ , that can be tolerated by the capacitor. We also introduce the concept of depth of discharge of the battery bank and denote it as  $d_b$ , which is calculated as follows:

$$d_b = 1 - s_b. \quad (6)$$

The DC bus collects the energy generated by both the wind and solar subsystems and delivers it to the water desalination system and, if necessary, to the battery bank as well as to the electrical grid. The voltage of the DC bus is determined by the battery bank.

We use a binary variable  $I_s$  to indicate the operating mode of the integrated system. When  $I_s = 1$ , the integrated system is connected to the electrical grid; and when  $I_s = 0$ , the integrated system works in standalone mode. Assuming an ideal voltage inverter, we can write an energy balance equation in the form of current balance as follows:

$$i_w + i_s = i_{RO} + I_s i_G + i_b \quad (7)$$

where  $i_{RO}$  and  $i_G$  are the currents injected to the RO water desalination system and the electrical grid, respectively.

### B. Water Desalination System Description

In the RO water desalination system, there is a high-pressure pump, a membrane module and a water storage tank. Salt water enters the pump, which is equipped with a variable frequency drive, and is pressurized to the feed pressure [5]. The pressurized salt water stream enters the membrane module where it is separated into a low-salinity product (or permeate) stream, and a high-salinity brine (or retentate) stream. The RO system model can be obtained via a mass balance taken around the entire system and an energy balance taken around the actuated re-

tentate valve, which involves one ODE describing the dynamics of the retentate flow velocity,  $v_r$ . The detailed mathematic modeling of the RO system can be found in [5]. Various control techniques can be applied using the valve resistance value ( $e_{vr}$ ) as the manipulated input.

In this work, we operate the RO system at energy optimal water recovery  $Y_{opt}$ , which implies that the ratio of the permeate flow velocity  $v_p$  to the feed flow velocity  $v_f$  is being adjusted in real time; please see [1] and [10] for discussions on how to compute and achieve the energy optimal water recovery in real time. Based on the Bernoulli equation and ignoring the water elevation change, we can obtain the power needed for the water desalination system as follows:

$$P_{RO} = \frac{1}{\eta} \left( P_{sys} \frac{F_p}{Y_{opt}} + \frac{1}{2} \frac{F_p^3}{Y_{opt}^3 A_p^2} \rho_w \right), \quad 0 < \eta < 1 \quad (8)$$

where  $\eta$  is the overall power efficiency of the pump of the RO desalination system,  $P_{sys}$  is the feed pressure,  $F_p$  is the permeate flow rate (i.e., desalinated water production rate which is used to satisfy the water consumption and storage demands),  $A_p$  is the pipe cross-sectional area and  $\rho_w$  is the fluid density. If we denote the water consumption demand as  $F_d$  and water storage demand as  $F_s$ , then we obtain the following equation from a steady-state mass balance:

$$0 = F_p - F_d - F_s. \quad (9)$$

Note that the water storage demand  $F_s$  can take positive or negative values.

Based on the (9), the dynamics of the water level in the storage tank,  $h_l$ , can be obtained as follows:

$$\dot{h}_l = \frac{F_s}{A_s} = \frac{A_p}{A_s} (v_f - v_r) - \frac{F_d}{A_s} \quad (10)$$

where  $A_s$  is the cross-sectional area of the water storage tank. Similarly, we define the state of storage (SOS),  $s_t$ , for the storage tank as follows:

$$s_t = \frac{h_l}{h_l^{\max}}$$

where  $h_l^{\max}$  is the maximum water level in the storage tank.

### C. Dynamics of the Integrated Wind/Solar/RO System

The dynamics of the integrated wind/solar/RO system can be written in the following compact form:

$$\dot{x} = f(x) + g(x)u \quad h(x) = 0 \quad (11)$$

where  $x = [i_q \ i_d \ w_e \ v_{pv} \ i_s \ v_c \ v_r \ h_l]^T$ ,  $u = [u_w \ u_{pv} \ e_{vr}]^T$ , and,  $f, g, h$  are nonlinear vector functions whose explicit forms are omitted for brevity. We note that the dynamics of the integrated system exhibits a two-time-scale behavior. Specifically, the dynamics of the states  $i_q, i_d, w_e, v_{pv}, i_s$  and  $v_r$  are relatively fast (in the order of seconds); and the dynamics of the states  $v_c$  and  $h_l$  are relatively slow (in the order of minutes). Based on this

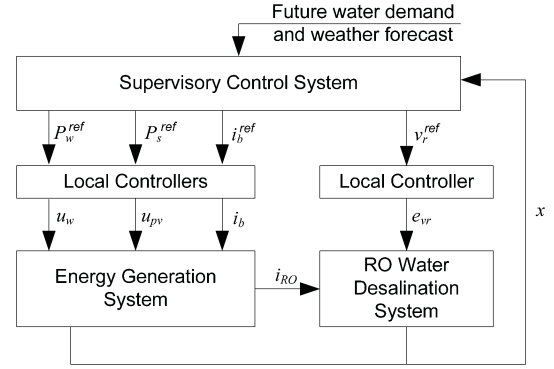


Fig. 2. Structure of the closed-loop system.

two-time-scale property, we can rewrite the integrated system of (11) as follows:

$$\begin{aligned} \dot{x}_f &= f_f(x_f, x_s) + g_f(x_f, x_s)u \\ \dot{x}_s &= f_s(x_f, x_s) \\ h(x) &= 0 \end{aligned} \quad (12)$$

where

$$f_s(x_f, x_s) = \left[ \begin{array}{c} \frac{1}{C_b} i_b \\ \frac{A_p}{A_s} (v_f - v_r) - \frac{F_d}{A_s} \end{array} \right]$$

and  $x_f = [i_q \ i_d \ w_e \ v_{pv} \ i_s \ v_r]^T$ ,  $x_s = [v_c \ h_l]^T$ . This two-time-scale property will be taken advantage of in the formulation of the supervisory MPC where the model of (12) with  $\dot{x}_f \equiv 0$  will be used.

## III. CONTROL PROBLEM FORMULATION AND CONTROLLER DESIGN

### A. Control Problem Formulation and Approach

In this section, we design the supervisory control system to regulate the integrated energy generation and RO water desalination system. The primary control objective is to regulate the integrated system to produce enough desalinated water to satisfy the total water consumption and storage demands. The secondary objective is to take into account optimality considerations on system operation, for example, battery maintenance and energy savings (so that more energy can be sent to the electrical grid). The supervisory control system computes the operating trajectories for all the subsystems in the integrated system. These operating trajectories are sent to the local controllers associated with the subsystems which force the subsystems to track the operating trajectories. A schematic of the structure of the closed-loop system is shown in Fig. 2.

### B. Design of Local Controllers

For the wind subsystem controller, the objective is to force the wind subsystem to track the operating trajectory, which is the desired power generation (power reference)  $P_w^{\text{ref}}$  computed by the supervisory control system. We follow the nonlinear controller design proposed in [11] to design the local controller for

the wind subsystem. For the solar subsystem controller, the objective is to force the solar subsystem to track the operating trajectory, which is the desired power generation  $P_s^{\text{ref}}$  computed by the supervisory controller. We follow the nonlinear controller design proposed in [9] to design this local controller. For the local controller associated with the RO water desalination, the objective is to regulate the retentate valve resistance to track the reference retentate flow velocity,  $v_r^{\text{ref}}$  computed by the supervisory controller. We adopt the method proposed in [5] to design a nonlinear model-based controller for the RO subsystem.

The supervisory control system also sends a reference charge/discharge current trajectory ( $i_b^{\text{ref}}$ ) to the battery bank; however, this reference is not always used in the local controller associated with the battery bank. From (7), we can see that in the cases where the integrated system operates in standalone mode (i.e.,  $I_s = 0$ ), and when there is no extra energy to send to the electrical grid and the system operates in grid-connected mode (i.e.,  $I_s = 1$  and  $i_G = 0$ ), the current across the battery bank is determined by the current balance which implies that the local controller associated with the battery bank is inactive. We assume that the local controller operates based on real-time measurements of  $i_w, i_s, i_{\text{RO}}$  and adopts the following control strategy:

$$i_b = \begin{cases} i_w + i_s - i_{\text{RO}}, & \text{if } I_s = 0 \\ \min\{i_b^{\text{ref}}, i_w + i_s - i_{\text{RO}}\}, & \text{if } I_s = 1. \end{cases} \quad (13)$$

The reader may refer to [12] for the design of controllers for battery banks.

### C. Supervisory Predictive Controller Design

The objective of the supervisory control system is to determine the operating power references ( $P_w^{\text{ref}}, P_s^{\text{ref}}$ ) for the wind and solar subsystems, the reference retentate flow rate ( $v_r^{\text{ref}}$ ) for the RO water desalination subsystem, and the charge/discharge current ( $i_b^{\text{ref}}$ ) of the battery bank. We propose to design the supervisory control system via MPC because it can take into account optimality considerations and handle state and input constraints.

In the supervisory MPC design, we explicitly account for the following considerations on the battery bank maintenance according to [12], [13].

- 1) Small charge/discharge currents are favorable, as large charge/discharge currents result in more energy dissipated in the battery internal resistance.
- 2) The charge current should be constrained under a certain upper bound which is a monotonically increasing function of the depth of discharge (DOD) of the battery bank. In this work, we set the upper bound of the charge currents based on a simple taper charging approach [12].
- 3) The DOD of the battery bank should not exceed  $d_b^{\text{max}}$  in order to protect the battery bank.
- 4) The battery should be charged if extra generated power is available (in addition to satisfying water production power demand).

To take into account energy savings considerations, we try to operate the RO water desalination subsystem at the energy optimal water recovery  $Y_{\text{opt}}$  so that the energy consumption of unit water production is minimized [1]. This implies that if the system is connected to the electrical grid, the energy sent

to the grid is maximized. In addition, we assume that there is a preferred SOS,  $s_t^{\text{opt}}$ , of the storage tank which is a balance between the capacities of the tank to supply unexpected water consumption demand and to store extra water production. We consider the case where the future water consumption demand of the RO subsystem is known; that is,  $F_d(t)$ , is known. We also assume that future hourly weather conditions (i.e., wind speed, insolation, photovoltaic cell temperature) forecast information is available.

The supervisory MPC is evaluated at discrete time instants  $t_k = t_0 + k\Delta, k = 0, 1, \dots$ , with  $t_0$  being the initial time and  $\Delta$  being the sampling time. At each sampling time, piece-wise constant trajectories of the operating trajectories of the different subsystems (i.e.,  $P_w^{\text{ref}}, P_s^{\text{ref}}, v_r^{\text{ref}}$ , and  $i_b^{\text{ref}}$ ) for a certain time period (prediction horizon) are obtained but only the first piece of the trajectories are sent to the local controllers and implemented. Note that the operating trajectories are restricted to belong to piece-wise constant functions in order to get finite dimensional MPC optimization problem. Before we discuss the formulation of the supervisory MPC, we present the cost function used in the MPC. Specifically, the proposed form of the cost function is as follows:

$$\begin{aligned} J(t) = & \alpha(1 - I_s) \int_0^{N\Delta} (P_{\text{RO}}(\tau) + i_b^{\text{ref}}(\tau)v_b(\tau) \\ & - P_w^{\text{ref}}(\tau) - P_s^{\text{ref}}(\tau))^2 d\tau \\ & + \beta(1 - I_s) \int_0^{N\Delta} \frac{P_s^{\text{ref}}(\tau)}{P_w^{\text{ref}}(\tau)} d\tau + \gamma \int_0^{N\Delta} d_b(\tau) d\tau \\ & + \epsilon \int_0^{N\Delta} (s_t(\tau) - s_t^{\text{opt}})^2 d\tau + \zeta \int_0^{N\Delta} i_b^{\text{ref}}(\tau)^2 d\tau \\ & + \theta \frac{\int_0^{N\Delta} P_{\text{RO}}(\tau) d\tau}{\int_0^{N\Delta} F_p(\tau) d\tau} + \kappa_1 \int_0^{N\Delta} \frac{I_s}{P_w^{\text{ref}}(\tau) + C_w} d\tau \\ & + \kappa_2 \int_0^{N\Delta} \frac{I_s}{P_s^{\text{ref}}(\tau) + C_s} d\tau \end{aligned} \quad (14)$$

where  $N$  is the prediction horizon of the MPC,  $\Delta$  is the sampling time,  $\alpha, \beta, \gamma, \epsilon, \zeta, \theta, \kappa_1$ , and  $\kappa_2$  are positive weighting factors, and  $C_w, C_s$  are positive constants. In this cost function, the first term, which is only active in standalone operating mode, is used to penalize the difference between the energy generated by the wind-solar system and the total power demand from the RO subsystem and the battery bank, thus driving the wind and solar subsystems to satisfy the total power demand to the maximum extent; the second term, which is also only active in standalone mode, implies that the wind subsystem is operated as the primary generation subsystem and the solar subsystem is activated when necessary; the third term implies that the battery should be charged if the battery is not fully charged; the fourth term is used to make sure that the water level in the storage tank is maintained around the optimal water level; the fifth term takes into account that small charge currents are preferred; the sixth term penalizes the power consumption per unit of permeate water produced; the last two terms are only activated when the integrated system is connected to the electrical grid, and force the wind and solar subsystems to operate at their maximum power generation points.

The proposed MPC design for the supervisory control system at time  $t_k$  is as follows:

$$\min_{P_w^{\text{ref}}, P_s^{\text{ref}}, i_b^{\text{ref}}, v_r^{\text{ref}} \in S(\Delta)} J(t_k) \quad (15a)$$

$$\text{s.t. } 0 \leq P_w^{\text{ref}}(\tau) \leq \min_{\tau} \{P_w^{\text{max}}(\tau)\}, \tau \in [t_{k+j}, t_{k+j+1}] \quad (15b)$$

$$0 \leq P_s^{\text{ref}}(\tau) \leq \min_{\tau} \{P_s^{\text{max}}(\tau)\}, \tau \in [t_{k+j}, t_{k+j+1}] \quad (15c)$$

$$F_p^{\text{min}} \leq F_p(\tau) \leq F_p^{\text{max}} \quad (15d)$$

$$0 \leq d_b(\tau) \leq d_b^{\text{max}} \quad (15e)$$

$$s_t^{\text{min}} \leq s_t(\tau) \leq s_t^{\text{max}} \quad (15f)$$

$$i_b^{\text{ref}}(\tau) \leq i_b^{\text{max}}(s_b(\tau)) \quad (15g)$$

$$\dot{\tilde{x}}_s(\tau) = f_s(\tilde{x}_f(\tau), \tilde{x}_s(\tau)) \quad (15h)$$

$$0 = f_f(\tilde{x}_f(\tau), \tilde{x}_s(\tau)) + g_f(\tilde{x}_f(\tau), \tilde{x}_s(\tau))u^{\text{ref}} \quad (15i)$$

$$h(\tilde{x}(\tau)) = 0 \quad (15j)$$

$$\tilde{x}_s(0) = x_s(t_k) \quad (15k)$$

where  $S(\Delta)$  denotes the family of piece-wise constant functions,  $j = 0, \dots, N - 1$ ,  $\tilde{x}$  is the predicted future state of the integrated system,  $x(t_k)$  is the state measurement at time  $t_k$ , and  $u^{\text{ref}}$  denotes the steady-state control inputs obtained based on the optimal references computed by the MPC.

The constraints of (15b) and (15c) require that the computed wind and solar subsystems' power references should be smaller than the minimum of the maximum available within each sampling interval, which means that the power references should be achievable for the wind and solar subsystems. Note that the future maximum available power for the wind and the solar subsystems are estimated using the information of future weather conditions forecast [9], [11]. The constraint of (15d) puts upper and lower bounds ( $F_p^{\text{max}}$  and  $F_p^{\text{min}}$ , respectively) on the permeate flow rate  $F_p$ , which is used to guarantee the equipment safety of the membrane module in the RO water desalination subsystem. The constraint of (15e) requires that the depth of discharge of the battery bank should not exceed  $d_b^{\text{max}}$ . The constraint of (15f) imposes upper and lower bounds on the water level in the storage tank. The constraint of (15g) places an upper bound on the charge current of the battery bank and this upper bound is a function of the current depth of discharge of the battery bank. Note that in the supervisory MPC design, only the slow system dynamics is taken into account [i.e., the constraints of (15h)–(15k)]; and the fast system states that are (explicitly or implicitly) used in the MPC are estimated by the computed future operating trajectories (decision variables of the MPC) [i.e., the constraint of (15i)]. For example, in the calculation of future  $F_p(\tau)$ , the fast state  $v_r$  is assumed to be equal to  $v_r^{\text{ref}}$ . Note also that in the implementation of the supervisory MPC, the order of the model used in the optimization problem of (15) may be further reduced by taking into account the specific structure of the system.

We denote the optimal solution to the optimization problem of (15) as  $P_w^{\text{ref},*}(\tau | t_k)$ ,  $P_s^{\text{ref},*}(\tau | t_k)$ ,  $i_b^{\text{ref},*}(\tau | t_k)$ , and  $v_r^{\text{ref},*}(\tau | t_k)$ . The references of power generation from the wind and solar subsystems, of battery charge/discharge current,

and of RO retentate flow rate sent to the local controllers by the supervisory controller of (15) are defined as follows:

$$\begin{aligned} P_w^{\text{ref}}(t) &= P_w^{\text{ref},*}(t | t_k), \quad \forall t \in [t_k, t_{k+1}] \\ P_s^{\text{ref}}(t) &= P_s^{\text{ref},*}(t | t_k), \quad \forall t \in [t_k, t_{k+1}] \\ i_b^{\text{ref}}(t) &= i_b^{\text{ref},*}(t | t_k), \quad \forall t \in [t_k, t_{k+1}] \\ v_r^{\text{ref}}(t) &= v_r^{\text{ref},*}(t | t_k), \quad \forall t \in [t_k, t_{k+1}]. \end{aligned} \quad (16)$$

Note that the constraints of (15b)–(15k) are inspired by results on the design of Lyapunov-based model predictive control systems (please see [14], [15]).

*Remark 1:* In this work, we consider that the integrated system already operates in normal operating conditions, and do not address the issues related to system startup or shut down. The stability of the system is ensured by the local controllers and the main purpose of the supervisory MPC is to coordinate the actions of the local controllers to improve the overall operation performance.

*Remark 2:* Note that in order to carry out real-time long-term (e.g., in the size of hours) optimization of the integrated wind/solar/RO system, it is essential to reduce the model used in the supervisory MPC formulation by taking into account the two-time-scale behavior of the integrated system. If a full system model is used in the MPC formulation, it is impossible to carry out real-time long-term optimization because very small integration step is required in order to get a stable and accurate numerical integration of the fast dynamics.

*Remark 3:* Note that the local controllers are standard (they do use the set-points computed by the supervisory controller). Even though the fast dynamics of the integrated system will have different transient behaviors when different local controllers are used, the performance of the supervisory MPC with different local controllers is not expected to exhibit significant differences because the supervisory MPC deals with the long-term behavior of the integrated system which is weakly dependent on the transient behavior of the fast dynamics.

#### IV. SIMULATION RESULTS

We carry out several sets of simulations to demonstrate the applicability and effectiveness of the supervisory MPC system for the integrated wind/solar/RO system. The prediction horizon and the sampling time of the MPC are chosen to be  $N = 24$  and  $\Delta = 1$  hr taking into account that the water demand (for example, of a community) usually presents periodic fluctuations with a period of 24 hr. The weighting factors in the cost function are chosen to be  $\alpha = 1.8 \times 10^{-7}$ ,  $\beta = 0.001$ ,  $\gamma = 0.001$ ,  $\epsilon = 0.01$ ,  $\zeta = 0.05 \times 10^{-9}$ ,  $\theta = 2 \times 10^{-7}$ ,  $\kappa_1 = 0.1$ , and  $\kappa_2 = 0.1$ . The values of the weighting factors of the different terms were determined through a trial-and-error approach. Note that in all the simulations, the optimization problem of the supervisory MPC is solved by the open source interior point optimizer Ipopt [16] and the average evaluation time of the supervisory MPC is about 7 s.

The overall RO system pump power efficiency is assumed to be  $\eta = 0.7$ , the upper bound on  $d_b$  is  $d_b^{\text{max}} = 0.8$ , the lower and upper bounds on  $F_p$  are  $F_p^{\text{min}} = 0.1814$  m<sup>3</sup>/hr and  $F_p^{\text{max}} = 3.9918$  m<sup>3</sup>/hr, respectively, and the lower and upper bounds on  $s_t$  are  $s_t^{\text{min}} = 0$  and  $s_t^{\text{max}} = 1$ , respectively. The upper bound

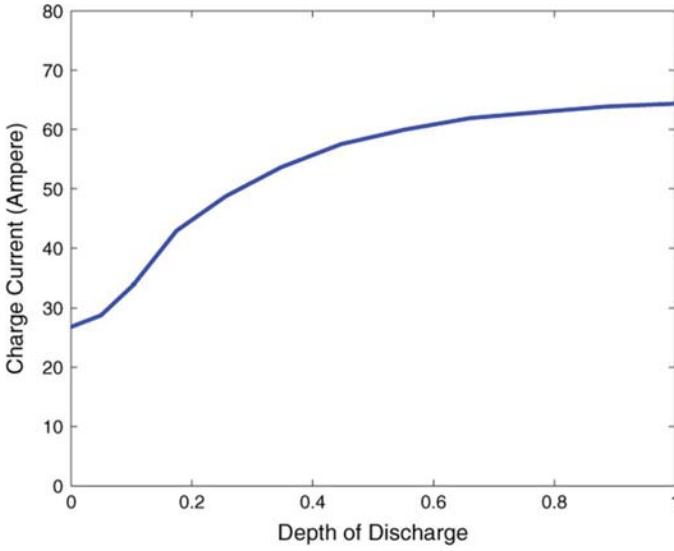


Fig. 3. Upper bound on battery charge current.

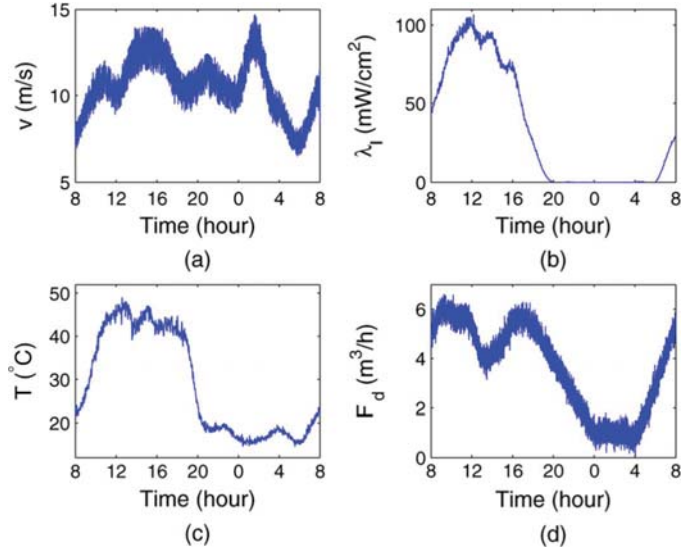


Fig. 5. Weather conditions and water demand. (a) Wind speed  $v$ . (b) insolation  $\lambda_l$ . (c) PV panel temperature  $T$ . (d) water demand  $F_d$ .

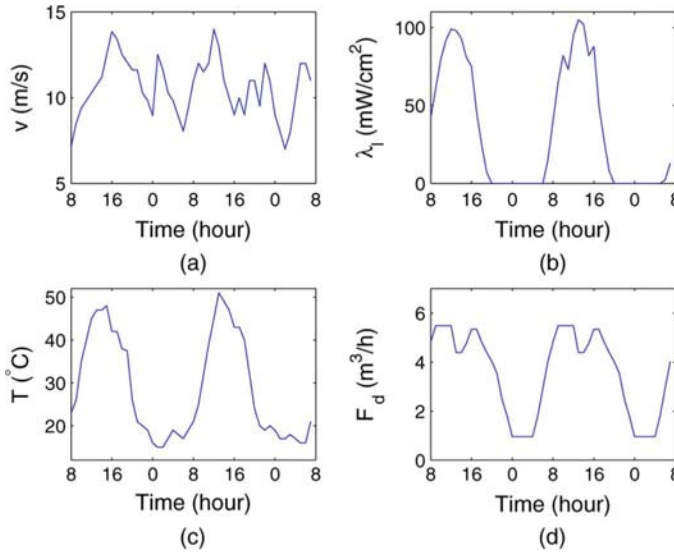


Fig. 4. Forecast of weather conditions and water demand. (a) Wind speed  $v$ . (b) insolation  $\lambda_l$ . (c) PV panel temperature  $T$ . (d) water demand  $F_d$ .

on the battery charge current is a function of  $d_b$  and is shown in Fig. 3.

We carry out simulations for one day starting at 8 am. In the simulations, we assume that weather forecast and water demand information of future 24 hr is available. We note that hourly weather condition forecast is available commercially and future water demand can be estimated based on previous water consumption data when the RO subsystem is used to provide water to a community. A two-day forecast of wind speed, insolation, PV cell temperature and water demand is shown in Fig. 4. We introduce hourly deviation and high frequency disturbances to the forecast information to simulate realistic fluctuations of weather and water demand for the first 24 hr, as shown in Fig. 5.

**A. Standalone Operating Mode**

In this subsection, we consider a standalone operating mode scenario ( $I_s = 0$ ), where the power generated by the wind/solar

subsystems can only be consumed by the RO water desalination subsystem and/or stored by the battery bank. In such a scenario, the references of the wind and solar subsystem power supply and retentate flow rate are optimized by the supervisory MPC, while the reference for the battery current is inactive in the MPC optimization problem and the current across the battery bank is determined by the current balance around the inverter as shown in (13).

Fig. 6 shows the time evolution of wind and solar subsystem power generation and RO subsystem power consumption. For each hour of operation, the wind/solar local controllers operate to drive the wind mill and the PV panel array to generate power according to the reference values, respectively. However, when the weather condition does not permit sufficient generation, for example during 15–21 hr and during 3–7 hr for the wind subsystem as shown in Fig. 6(a), the local controller switches to the operation mode of maximum power point tracking. In Fig. 6(c), when wind/solar power delivery alone cannot meet the RO power demand such as during 8–13 hr and during 4–8 hr, the battery discharges current to compensate for the shortfall; at other times, extra power generation is used to charge the battery.

An advantage of the supervisory MPC is that it is able to schedule the water production to be smooth (nearly uniform with respect to time) by taking into account future state variation and by coordinating the subsystems. It can be seen from Fig. 7(a) that water production is relatively smooth despite dramatically varying water demand and weather conditions during a day. This is largely due to the optimized utilization of the capacities of the battery bank and of the water tank which act as buffers against external fluctuations. The state of charge of the battery bank and the state of storage of the water tank are shown in Fig. 7(b).

**B. Electrical Grid-Connected Operating Mode**

Next we carry out simulations where the integrated wind/solar/RO system is operated in electrical grid-connected mode

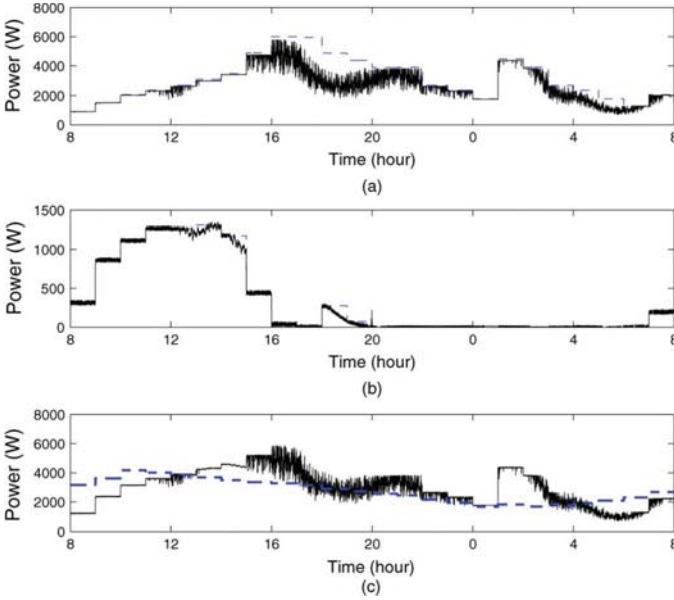


Fig. 6. Power generation and consumption in the standalone operating mode. (a) Power generated by wind subsystem  $P_w$  (solid line) and wind power reference  $P_{w,ref}$  (dashed line). (b) Power generated by solar subsystem  $P_s$  (solid line) and solar power reference  $P_{s,ref}$  (dashed line). (c) Generated power  $P_w + P_s$  (solid line) and total power demand  $P_{RO}$  (dashed line).

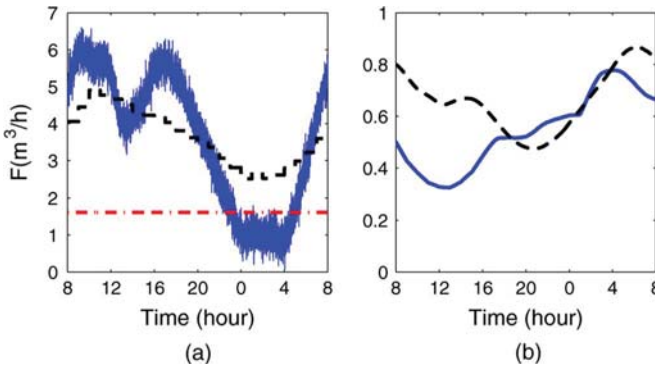


Fig. 7. (a) Rate of water demand  $F_d$  (solid line) and permeate flow rate  $F_p$  (dashed line). (b) Battery state of charge  $s_b$  (solid line) and tank state of storage  $s_t$  (dashed line).

( $I_s = 1$ ). In this case, the supervisory MPC forces the wind/solar subsystems to track the maximum power generation points all the time and optimizes the trajectories of battery current and retentate flow rate at each sampling interval.

In this subsection, we compare the proposed supervisory MPC with a reference control strategy which does not take into account optimality considerations. The reference control strategy is as follows:

- 1) the wind/solar subsystems track their maximum power generation points all the time;
- 2) if the tank state of storage exceeds 0.8, the RO water desalination subsystem produces water at  $F_p = F_p^{\min}$ ; if it is below 0.6, the RO water desalination subsystem produces

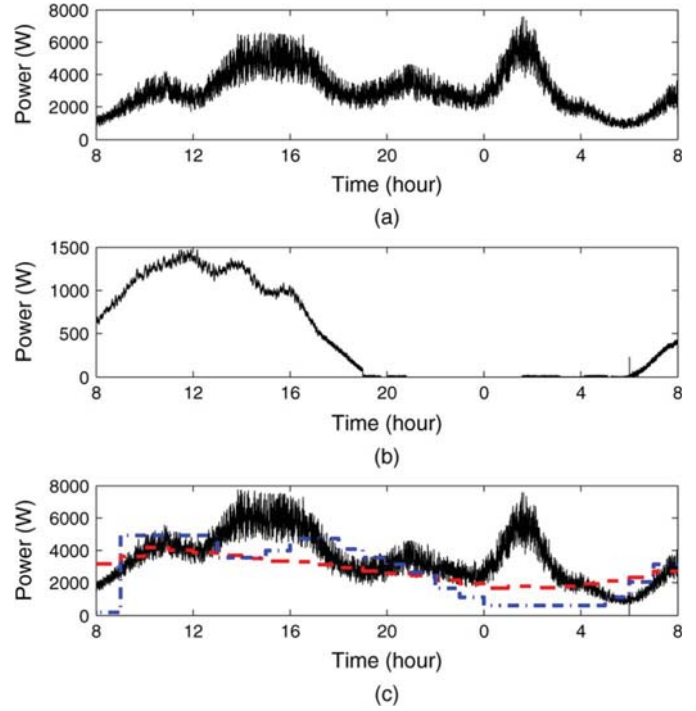


Fig. 8. (a) Power generated by the wind subsystem  $P_w$ . (b) Power generated by the solar subsystem  $P_s$ . (c) Generated power  $P_w + P_s$  (solid line) and total power demand  $P_{RO}$  under the supervisory MPC (dashed line) and under the reference control strategy (dashed-dotted line).

water at  $F_p = F_p^{\max}$ ; else the RO water desalination subsystem produces water according to the forecast average water demand of the next hour;

- 3) if necessary, extra produced energy is first used to charge the battery bank; and when the battery bank is fully charged or the charge current hits the upper bound, the extra produced energy is sent to the electrical grid.

The simulation results under the supervisory MPC and the reference control are shown in Figs. 8 and 9. From Figs. 8(c) and 9(a), it can be seen that the RO water desalination has a smoother water production under the supervisory MPC compared with that under the reference control, which results in reduced average energy consumption as shown in Fig. 9(b). In the time periods from 13–14 hr and from 22–7 hr, the power consumption per unit water production (denoted as  $Q_u$ ) under the simple reference control is less than that under the supervisory MPC because the permeate flow rate with the former is closer to the optimal level. However, during the first hour and the period from 0–5 hr, the reference control operates the RO subsystem with a permeate flow rate below the optimal value, which results in low water production and relatively high power consumption. For the entire day, the average power consumption per cubic meter of water production is  $2.94 \times 10^6$  J/m<sup>3</sup> under the reference control and is  $2.74 \times 10^6$  J/m<sup>3</sup> under the supervisory MPC, which is 7.06% less than that under the reference control strategy.

In addition, we compare the battery charge/discharge currents under the supervisory MPC and the reference control as shown in Fig. 10. As a result of optimization considerations for battery

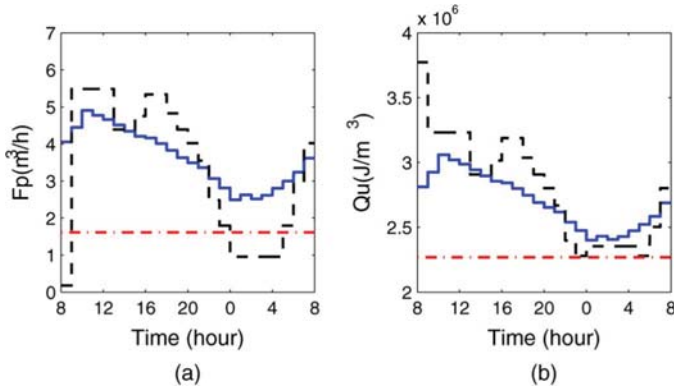


Fig. 9. (a) Permeate flow rate  $F_p$  under the supervisory MPC (solid line) and the reference control strategy (dashed line), and  $F_p$  corresponding to the minimum power consumption per unit water production (dashed-dotted line). (b) Power consumption per cubic meter of water production  $Q_u$  under the supervisory MPC (solid line) and under the reference control strategy (dashed line), and the corresponding minimum power consumption (dashed-dotted line).

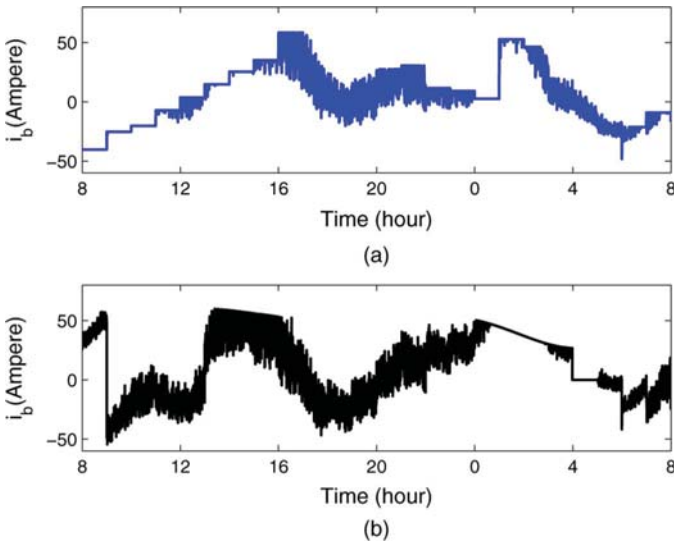


Fig. 10. (a) Battery charge/discharge current with supervisory MPC. (b) Battery charge/discharge current with the reference strategy.

maintenance, it is evident that the charge/discharge process is smoother under the supervisory MPC.

Finally, we study the dependence of the performance of the supervisory MPC on the future weather and water demand forecast information. We consider two different cases. The first case is that we only have water demand forecast information for the next hour and the daily average water demand instead of the future 24-hr forecast information; the second case is that we only have access to weather conditions forecast information for the next hour and the corresponding wind speed daily average value, insolation and PV cell temperature daytime and nighttime average values. The evolutions of the permeate flow rate and of the corresponding power consumption per unit water production for the two cases are shown in Fig. 11(a) and (b), respectively. It can be observed that the permeate flow rate trajectory in the case of less water demand forecast deviates from the trajectory obtained with 24-hr weather and water demand forecast information available, while that in the case of less weather forecast

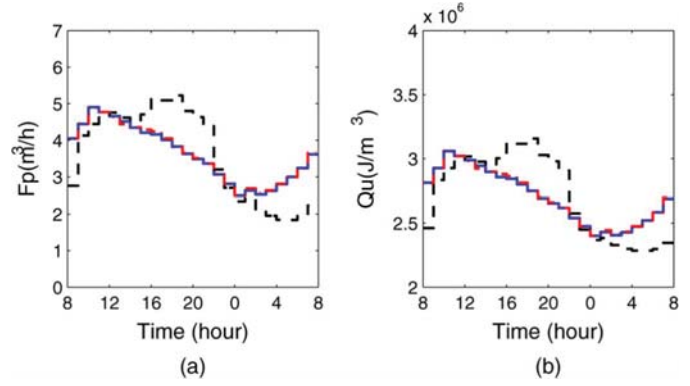


Fig. 11. (a) Permeate flow rate  $F_p$  under the supervisory MPC with future 24-hr forecast weather conditions and water demand information available (solid line), with only 1-hr water demand forecast and 24-hr weather forecast information available (dashed line) and with only 1-hr weather forecast and 24-hr water demand forecast information available (dashed-dotted line). (b) Power consumption per cubic meter of water production  $Q_u$  under the supervisory MPC with future 24-hr forecast weather conditions and water demand information available (solid line), with only 1-hr water demand forecast and 24-hr weather forecast information available (dashed line) and with only 1-hr weather forecast and 24-hr water demand forecast information available (dashed-dotted line).

information almost overlaps with the trajectory obtained with 24-hr weather and water demand forecast information available. Moreover, the average power consumption per cubic meter of water production in the first and the second cases exceed the case with 24-hr forecast information available by 2.92% and less than 0.1%, respectively. From this set of simulations, we found that the performance of the supervisory MPC has stronger dependence on the forecast of future water demand than on the forecast of future weather information.

*Remark 4:* In the simulations, we compared the performance of the proposed supervisory MPC with that of an intuitive and standard reference control strategy. We note that the use of linear control (or of other control strategies) at the supervisory layer would potentially lead to improved results over the standard reference strategy but still it would not make possible the incorporation of constraints and complex cost functions in the control problem formulation and solution, as it is done with the proposed supervisory MPC. We also note that linear MPC could also be used as the supervisory control system but the system model is nonlinear and repeated linearization would be required to implement linear MPC.

### V. CONCLUSION

In this work, a supervisory MPC was designed to optimally operate an integrated wind/solar/RO system. The supervisory MPC is able to coordinate the wind/solar subsystems and the battery to provide enough energy to the RO subsystem to meet desired water production demand. Optimality considerations on system operation and energy savings were also taken into account. Moreover, in the supervisory MPC design, the two-time-scale property of the dynamics of the integrated system was considered to improve the computational efficiency. Simulations were carried out to illustrate the applicability and effectiveness of the proposed supervisory MPC. In our future work, we will consider distributed control of renewable energy generation systems connected to the electrical grid.

## REFERENCES

- [1] A. Zhu, A. Rahardianto, P. D. Christofides, and Y. Cohen, "Reverse osmosis desalination with high permeability membranes-cost optimization and research needs," *Desalination Water Treatment*, vol. 15, pp. 256–266, 2010.
- [2] C. Charcosset, "A review of membrane processes and renewable energies for desalination," *Desalination*, vol. 245, pp. 214–231, 2007.
- [3] M. Chinchilla, S. Arnaltes, and J. C. Burgos, "Control of permanent-magnet generators applied to variable-speed wind-energy systems connected to the grid," *IEEE Trans. Energy Convers.*, vol. 21, no. 1, pp. 130–135, Mar. 2006.
- [4] N. Hamrouni, M. Jraidi, and A. Cherif, "New control strategy for 2-stage grid-connected photovoltaic power system," *Renewable Energy*, vol. 33, pp. 2212–2221, 2008.
- [5] A. R. Bartman, P. D. Christofides, and Y. Cohen, "Nonlinear model-based control of an experimental reverse-osmosis water desalination system," *Ind. Eng. Chem. Res.*, vol. 48, pp. 6126–6136, 2009.
- [6] W. Qi, J. Liu, X. Chen, and P. D. Christofides, "Supervisor predictive control of stand-alone wind-solar energy generation systems," *IEEE Trans. Control Syst. Technol.*, vol. 19, no. 1, pp. 199–207, Jan. 2011.
- [7] D. Q. Mayne, J. B. Rawlings, C. V. Rao, and P. O. M. Scokaert, "Constrained model predictive control: Stability and optimality," *Automatica*, vol. 36, pp. 789–814, 2000.
- [8] F. Valenciaga, P. F. Puleston, P. E. Battaiotto, and R. J. Mantz, "Passivity/sliding mode control of a stand-alone hybrid generation system," *IEE Proc. Control Theory Appl.*, vol. 147, pp. 680–686, 2000.
- [9] F. Valenciaga, P. F. Puleston, and P. E. Battaiotto, "Power control of a photovoltaic array in a hybrid electric generation system using sliding mode techniques," *IEE Proc. Control Theory Appl.*, vol. 148, pp. 448–455, 2001.
- [10] A. Zhu, P. D. Christofides, and Y. Cohen, "Effect of thermodynamic restriction on energy cost optimization of RO membrane water desalination," *Ind. Eng. Chem. Res.*, vol. 48, pp. 6010–6021, 2009.
- [11] F. Valenciaga, P. F. Puleston, and P. E. Battaiotto, "Variable structure system control design method based on a differential geometric approach: Application to a wind energy conversion subsystem," *IEE Proc. Control Theory Appl.*, vol. 151, pp. 6–12, 2004.
- [12] , D. Linden and T. B. Reddy, Eds., *Handbook of Batteries*, 3rd ed. New York: McGraw-Hill, 2002.
- [13] A. J. Ruddell, A. G. Dutton, H. Wenzl, C. Ropeter, D. U. Sauer, J. Merten, C. Orfanogiannis, J. W. Twidell, and P. Vezin, "Analysis of battery current microcycles in autonomous renewable energy systems," *J. Power Sources*, vol. 112, pp. 531–546, 2002.
- [14] P. D. Christofides and N. H. El-Farra, *Control of Nonlinear and Hybrid Process Systems: Designs for Uncertainty, Constraints and Time-Delays*. Berlin, Germany: Springer-Verlag, 2005.
- [15] P. Mhaskar, N. H. El-Farra, and P. D. Christofides, "Stabilization of nonlinear systems with state and control constraints using Lyapunov-based predictive control," *Syst. Control Lett.*, vol. 55, pp. 650–659, 2006.
- [16] A. Wächter and L. T. Biegler, "On the implementation of primal-dual interior point filter line search algorithm for large-scale nonlinear programming," *Math. Program.*, vol. 106, pp. 25–57, 2006.